

Subspace Detection of the Impulse Response Function from Intrapartum Uterine Pressure and Fetal Heart Rate Variability

Philip A Warrick¹, Emily F Hamilton^{1,2}

¹ PeriGen, Inc, Montreal, Canada

² Department of Obstetrics and Gynecology, McGill University, Montreal, Canada

Abstract

Using clinically measured intrapartum cardiotocography (CTG) data, the objective of this study was to detect the impulse response function (IRF) of the single-input single-output system composed of uterine pressure as the input and one of three frequency band powers of fetal heart rate variability (fHRV) as the output. The results showed statistically significant differences between normal fetuses and those that had developed metabolic acidosis. This occurred in all frequency bands, with more differences occurring in the higher bands. These results are very promising for the improved detection of fetal distress related to hypoxia.

1. Introduction

Labour and delivery is routinely monitored electronically with sensors that measure and record maternal uterine pressure (UP) and fetal heart rate (FHR), a procedure referred to as cardiotocography (CTG). The objective of this monitoring is to detect the fetus at substantial risk of hypoxic injury so that intervention can prevent its occurrence.

In previous work [1, 2], we studied the deceleration response to contraction, which can be considered the dominating and lowest frequency component response to contraction. In this study, we shift the focus to the response to contraction of higher frequency FHR components ($> 30\text{mHz}$), often referred to as fetal heart rate variability (fHRV), and use UP and and input and fHRV as the output for system identification modelling.

To do so, we first estimated the fHRV using an autoregressive model of the CTG FHR signal to estimate the power spectral density (PSD), as described in [3]. The PSD was integrated over low frequency (LF, 30-150 mHz) and movement frequency (MF, 150-500 mHz) and high frequency (HF, 500-1000 mHz) bands to obtain three instantaneous components of fHRV.

We then performed linear system identification over

20 min epochs using the CTG uterine pressure (UP) as an input and each of the fHRV components as an output. The previous PSD step, therefore, can be considered as a linearization of the problem, which allows powerful linear methodologies to be used. This is important because estimating this system is a challenge with noisy CTG data, which often contains sensor artifacts and maternal FHR interference. We used the *PO-MOESP* subspace system identification approach [4], as it is well-suited to these conditions.

This work is related to that of a study on a small sample of healthy fetuses, which found that there were FHR responses to contractions at frequencies quite different from the contractions themselves, and with frequency-dependent lags [5]. However, our study is the first to quantify the nonlinear UP-fHRV relationship using system identification and draws from a much larger and varied population of fetuses in order to attempt to draw conclusions about the discriminatory power of this approach.

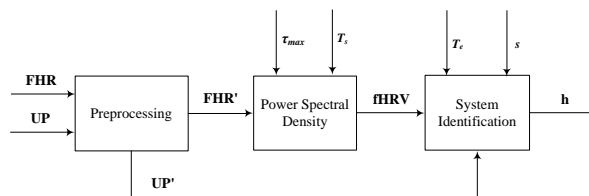


Figure 1. Block diagram of overall processing

2. Methods

2.1. Data

The data consisted of 231 cardiotocography (CTG) recordings of singleton, term pregnancies having no known congenital malformations, with at least three hours of tracing just prior to delivery. Each tracing was labelled by outcome information available after delivery (blood gases and

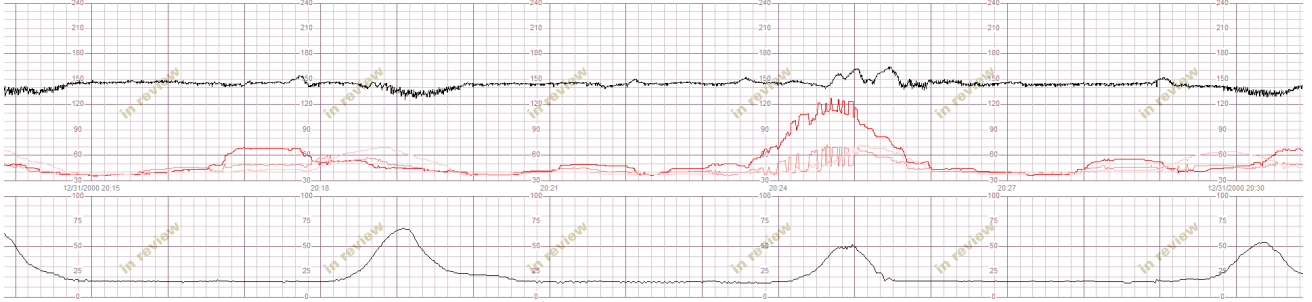


Figure 2. From a typical metabolic acidosis (M) case, acquired FHR and UP signals (in black, top and bottom respectively) as well as the computed instantaneous fHRV components (LF, MF and HF bands are in dark red, pink and lighter pink, respectively). The acquired signals are to scale with the units as shown (30 to 240 bpm), but the fHRV signals have been magnified for clarity (their vertical scales have limits of 0 and 10 bpm).

neurological assessment). 89 of the cases were normal (N) while 142 had developed metabolic acidemia (M)

Data collection was performed by clinicians using standard clinical fetal monitors to acquire the CTG. The monitors reported at uniform sampling rates of 4 Hz for FHR (measured in beats per minute (bpm)) and 1 Hz for UP (measured in mmHg). In the majority of cases, the UP or FHR sensors were attached to the maternal abdomen; the FHR was acquired from an ultrasound probe and the UP was acquired by tocography. In a few cases, they were acquired internally via an intra-uterine (IU) probe and/or a fetal-scalp electrode.

2.2. Overall approach

As shown in Fig. 1 the acquired UP and FHR signals were preprocessed to interpolate missing data and remove very low-frequency trends (< 30 mHz). Using short-term ($\tau_{\max}=1$ min) autoregressive models constructed at $T_s=1$ s increments, power spectral density (PSD) estimates were computed and the spectrum was integrated over low frequency (LF, 30-150 mHz) and movement frequency (MF, 150-500 mHz) and high frequency bands (HF, 500-1000 mHz) to obtain three instantaneous components of fHRV, which were down-sampled to 0.5 Hz. Using overlapping $T_e=20$ min epochs, and using the UP as the input and each of the HRV components as outputs, subspace system identification with scaling factor s was used to estimate impulse response functions \mathbf{h} .

2.3. Preprocessing

The CTG data was recorded in a clinical setting, so it was subject to specific types of noise. The loss of sensor contact can temporarily interrupt the UP or FHR signals, and interference from the (much lower) maternal heart rate can corrupt the FHR. These both appeared in the signal as a sharp drop to much lower amplitude followed by a sharp

signal restoration. We preprocessed the data to bridge these interruptions with linear interpolation.

The UP and FHR were then detrended by a high-pass filter with cutoff frequency 30 mHz, corresponding to the lower limit of the LF band of fetal HRV [6]. In addition, the UP was down-sampled to 0.5 Hz.

2.4. Power spectral density (PSD)

We computed a power spectral density using an autoregressive model using an approach similar to that taken in [2], except that all bridged intervals were excluded from consideration in the autocorrelation estimation to reduce bias introduced by the linear interpolation. The amount of missing data was monitored to provide subsequent assessment of the confidence in the PSD estimates.

We modified the calculation of the conventional FHR autocorrelation estimate r_f to exclude the intervals where the signal had been interpolated in the preprocessing step. Therefore, the revised estimate for a window of n samples was:

$$r_f(k) = \frac{1}{n_k} \sum_{i=0}^{n-1} \sum_{k=0}^{N-1} f(i)f(i-k) \quad (1)$$

where N is the longest lag and each term $f(i)f(i-k)$ is included in the sum if and only if both $f(i)$ and $f(i-k)$ are non-interpolated samples and n_k is the total number of $f(i)f(i-k)$ terms included at lag k .

Similar to the method described in [2], we used the autocorrelation estimates to compute coefficients of an AR model using linear prediction via the Levinson-Durbin algorithm and chose the model order p using the minimum-description length (MDL) criterion. Power spectral densities (PSD) of the AR models were computed following [7] and sampled at 128 frequencies between 0 and the Nyquist frequency of 2 Hz to resolve the dominant resonances.

We estimated successive PSDs of the fHRV at intervals of $T_s=1$ s using a maximum lag $\tau_{\max}=1$ min of the autocorrelation function r_f . At each time interval j , the LF and MF PSD bands were summed to give instantaneous bands estimates $fHRV_{LF}(j)$, $fHRV_{MF}(j)$ and $fHRV_{HF}(j)$. The square-root magnitude of these band sums were computed to transform them to bpm units for more convenient comparison with the acquired FHR. These estimates were down-sampled to 0.5 Hz in preparation for system identification.

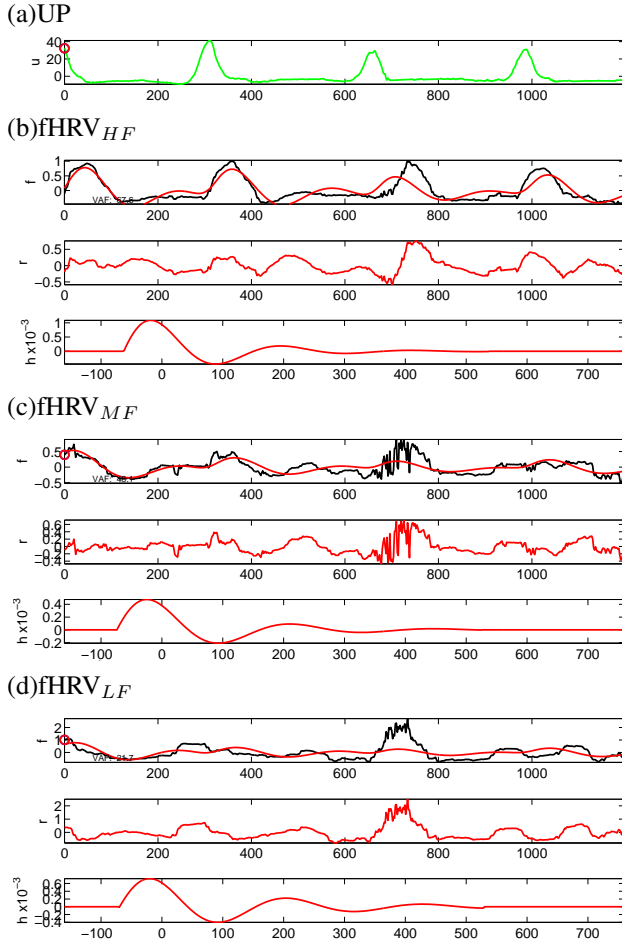


Figure 3. System identification results for the epoch from Fig. 2. Uterine Pressure (UP) is shown in (a). For each of the HF, MF and LF bands, (b), (c) and (d) show calculated HRV (black) and model-predicted HRV (red) followed by the residual r in the second panel, followed by the IRF estimate in the third panel, shifted to the left by the width of the autocorrelation window (60 s). The model parameters were: LF Gain: 0.017 bpm/mmHg, LF delay: -12 s, LF VAF: 21.7% MF Gain: 0.012 bpm/mmHg, MF delay: -16 s, MF VAF: 48.1% HF Gain: 0.026 bpm/mmHg, HF delay: -4 s, HF VAF: 77.6%

2.5. System identification

Subspace methods are well-suited to the noisy data of this problem because of their inherent singular-value decomposition and the fact that they permit non-contiguous data to be included in the estimation. We used the *PO-MOESP* subspace method [4] to estimate second-order (two-dimensional state) state-space system models. We chose a *PO-MOESP* scaling factor s of 64 samples = 128 s to be greater than the autocorrelation window size and therefore sensitive to longer dynamics.

Because of UP periodicity, there was no unique system model; we searched for a best model by shifting the output signal with respect to the input to find an IRF beginning with a first coefficient near 0. The associated shift represented the delay of the output response relative to the input onset. A negative delay indicated that the response preceded the input (due to UP measurement delay).

3. Results

Fig. 2 shows the acquired UP and FHR signals as well as the fHRV components over a typical epoch from an M case. It is clear that the fHRV components are relatively flat between the peaks of the UP (i.e. the uterine contractions), while the components generally peak in response to the uterine contraction. The LF components tend to dominate the MF and HF components, but their time courses are similar.

For this same epoch, Fig. 3 shows the system identification inputs UP and outputs $fHRV_{LF}$, $fHRV_{MF}$, $fHRV_{HF}$ and the corresponding IRF models and predicted outputs.

We then examined the time course of the IRF delay between between N and M classes over the last three hours of labour and delivery. Fig. 4 shows that compared to the N cases, the M cases had delays that were consistently higher. Specifically, there were statistically significant class differences in 3 epochs (HF band), 2 epochs (MF band) and 1 epoch (LF band), respectively. The onset of these differences occurred roughly 90 minutes before delivery in each case. We also computed the IRF steady-state gain G as the sum of the IRF coefficients $G = \sum_{i=0}^{M-1} h_i$, but this parameter did not show statistically significant differences between classes.

4. Conclusions

The IRF delay estimates from system identification modelling discriminated healthy fetuses from those who had developed metabolic acidosis and did so early (~ 90 min) with respect to delivery. This is important since these cases can be considered “near misses”: although they suffered the effects of hypoxia, the insult was not severe enough in intensity or duration to cause injury. Therefore,

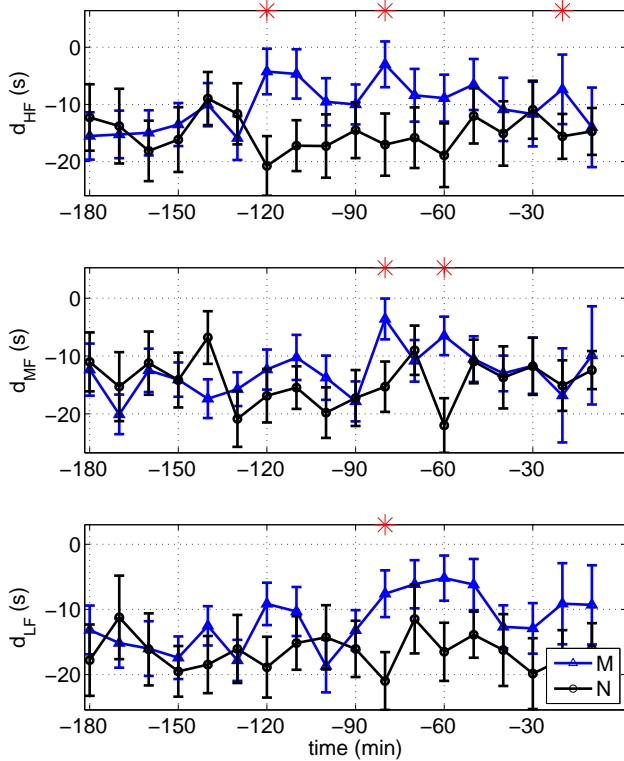


Figure 4. Delays of the impulse response function from subspace system identification using uterine pressure as an input and three bands of fetal heart rate variability (fHRV) as outputs: (a) low frequency (LF) (b) movement frequency (MF) and (c) high frequency (HF). The horizontal axis is the time in minutes with respect to delivery and the vertical axis is the delay in seconds. The means are plotted with bars indicating standard error and the red asterisks indicating statistically significant differences between normal (black circles) and metabolic acidotic (blue triangles) cases at that epoch ($p < 0.05$, Kolmogorov-Smirnov distribution test).

these are promising results for the early detection of fetal distress, before injury occurs, and in time to respond with appropriate clinical intervention (such as cesarian section).

The finding that delays from higher frequency bands were more often discriminating may be useful for future research, since different neural mechanisms exist for lower

bands, where sympathetic activity dominates, compared to higher bands, where parasympathetic activity dominates.

It is significant that we observed these band-specific differences despite the rather poor HF band HRV measurements that are possible using clinical, Doppler-based FHR. We expect that new measurement techniques providing accurate R-R intervals will further improve the HF HRV estimates and accordingly, the discrimination possible from this technique.

References

- [1] Warrick PA, Hamilton EF, Precup D, Kearney RE. Identification of the dynamic relationship between intra-partum uterine pressure and fetal heart rate for normal and hypoxic fetuses. *IEEE Transactions on Biomedical Engineering* June 2009;56(6):1587–1597.
- [2] Warrick PA, Hamilton EF, Precup D, Kearney R. Classification of normal and hypoxic fetuses from systems modeling of intrapartum cardiocography. *IEEE Transactions on Biomedical Engineering* 2010;57(4):771–779. ISSN 0018-9294.
- [3] Warrick PA, Hamilton EF. Fetal heart-rate variability response to uterine contractions during labour and delivery. In *Computing in Cardiology*, volume 39. 2012; 417–420.
- [4] Verhaegen M, Verdult V. *Filtering and system identification: a least squares approach*. Cambridge, UK.: CUP, 2007.
- [5] Romano M, Bifulco P, Cesarelli M, Sansone M, Bracale M. Foetal heart rate power spectrum response to uterine contraction. *Medical and Biological Engineering and Computing* March 2006;44:88–201.
- [6] Signorini M, Magenes G, Cerutti S, Arduini D. Linear and nonlinear parameters for the analysis of fetal heart rate signal from cardiocographic recordings. *IEEE Transactions on Biomedical Engineering* 2003;50(3):365–374. ISSN 0018-9294.
- [7] Cerutti S, Civardi S, Bianchi A, Signorini M, Ferrazzi E, Pardi G. Spectral analysis of antepartum heart rate variability. *Clin Phys Physiol Meas* 1989;10:27–31.

Address for correspondence:

Philip A. Warrick
 PeriGen Inc. (Canada)
 245 Victoria Avenue, suite 600
 Montreal, Quebec H3Z 3M6 Canada
 philip.warrick@perigen.com